

First-principles study on stability and superconductivity of ternary hydride $LaYH_x$(x=2, 3, 6 and 8)

Xiao-Zhen Yan(颜小珍), Xing-Zi Zhou(周幸姿), Chao-Fei Liu(刘超飞), Yin-Li Xu(徐寅力), Yi-Bin Huang(黄毅斌), Xiao-Wei Sheng(盛晓伟), and Yang-Mei Chen(陈杨梅)
Citation: Chin. Phys. B, 2024, 33 (**8**): 086301. DOI: 10.1088/1674-1056/ad41b8

What follows is a list of articles you may be interested in

New carbon-nitrogen-oxygen compounds as high energy density materials

Junyu Shen(沈俊宇), Qingzhuo Duan(段青卓), Junyi Miao(苗俊一), Shi He(何适),Kaihua He(何开华), Wei Dai(戴伟), and Cheng Lu(卢成)
Chin. Phys. B, 2023, 32 (**9**): 096302. DOI: 10.1088/1674-1056/acce94

Boron at tera-Pascal pressures

Peiju Hu(胡佩菊), Junhao Peng(彭俊豪), Xing Xie(谢兴), Minru Wen(文敏儒),Xin Zhang(张欣), Fugen Wu(吴福根), and Huafeng Dong(董华锋)
Chin. Phys. B, 2022, 31 (**3**): 036301. DOI: 10.1088/1674-1056/ac11e6

Inverted V-shaped evolution of superconducting temperature in SrBC under pressure

Ru-Yi Zhao(赵如意), Xun-Wang Yan(闫循旺), and Miao Gao(高淼)
Chin. Phys. B, 2021, 30 (**7**): 076301. DOI: 10.1088/1674-1056/abfbcc

Review of thermal transport and electronic properties of borophene

Dengfeng Li(李登峰), Ying Chen(陈颖), Jia He(何佳), Qiqi Tang(汤琪琪), Chengyong Zhong(钟承勇), Guangqian Ding(丁光前)
Chin. Phys. B, 2018, 27 (**3**): 036303. DOI: 10.1088/1674-1056/27/3/036303

The superconducting properties of a Pb/$MoTe_2$/Pb heterostructure:First-principles calculations within the anisotropic Migdal-Eliashberg theory

Wei Xia(夏威), Jie Zhang(张洁), Gui-Qin Huang(黄桂芹)
Chin. Phys. B, 2018, 27 (**12**): 126302. DOI: 10.1088/1674-1056/27/12/126302

First-principles study on stability and superconductivity of ternary hydride $LaYH_x$ ($x = 2$, 3, 6 and 8)

Xiao-Zhen Yan(颜小珍)[1], Xing-Zi Zhou(周幸姿)[1], Chao-Fei Liu(刘超飞)[1], Yin-Li Xu(徐寅力)[1], Yi-Bin Huang(黄毅斌)[1], Xiao-Wei Sheng(盛晓伟)[2,3], and Yang-Mei Chen(陈杨梅)[1,†]

[1] *School of Science, Jiangxi University of Science and Technology, Ganzhou* 341000, *China*
[2] *Department of Physics, Anhui Normal University, Wuhu* 241000, *China*
[3] *Anhui Province Key Laboratory of Optoelectric Materials Science and Technology, Wuhu* 241000, *China*

(Received 25 February 2024; revised manuscript received 22 April 2024; accepted manuscript online 23 April 2024)

Recent studies have shown that the La- and Y-hydrides can exhibit significant superconducting properties under high pressures. In this paper, we investigate the stability, electronic and superconducting properties of $LaYH_x$ ($x = 2$, 3, 6 and 8) under 0–200 GPa. It is found that $LaYH_2$ stabilizes in the $C2/m$ phase at ambient pressure, and transforms to the $Pmmn$ phase at 67 GPa. $LaYH_3$ stabilizes in the $C2/m$ phase at ambient pressure, and undergoes phase transitions of $C2/m \rightarrow P2_1/m \rightarrow R3m$ at 12 GPa and 87 GPa, respectively. $LaYH_6$ stabilizes in the $P4_32_12$ phase at ambient pressure, and undergoes phase transitions of $P4_32_12 \rightarrow P4/mmm \rightarrow Cmcm$ at 28 GPa and 79 GPa, respectively. $LaYH_8$ stabilizes in the $Imma$ phase at 60 GPa and transforms to the $P4/mmm$ phase at 117 GPa. Calculations of the electronic band structures show that the $P4/mmm$-$LaYH_8$ and all phases of $LaYH_2$ and $LaYH_3$ exhibit metallic character. For the metallic phases, we then study their superconducting properties. The calculated superconducting transition temperatures (T_c) are 0.47 K for $C2/m$-$LaYH_2$ at 0 GPa, 0 K for $C2/m$-$LaYH_3$ at 0 GPa, and 55.51 K for $P4/mmm$-$LaYH_8$ at 50 GPa.

Keywords: superconductivity, high pressure, first-principles study, phase transitions

PACS: 74.70.–b, 62.50.–p, 63.20.dk, 87.15.Zg **DOI:** 10.1088/1674-1056/ad41b8

1. Introduction

Superconducting materials are of great interest due to the economic value they can bring to various applications. According to the BCS theory,[1] metallic hydrogen is considered as a potential high-temperature (T_c) superconductor. Researchers proposed through theoretical calculations that metallic hydrogen can be obtained at a pressure of 495 GPa.[2] However, the exceptionally high-pressure requirement limits the experimental synthesis of metallic hydrogen. Ashcroft predicted that hydrogen-rich compounds can reach metallic state at much lower pressures due to the effect of chemical "precompression".[3] Ashcroft's theory was supported by subsequent findings of superconducting hydrides.[4–6]

So far, researchers have studied binary hydrides thoroughly and found many superconducting hydrides with T_c up to 200 K,[4–7] such as CaH_6,[8] LaH_{10}[9] and YH_6.[10] They exhibit common features: hydrogen atoms are weakly covalently bonded to each other to form a hydrogen cage and the structure is highly symmetric. The strong electron–phonon coupling of the H-cage contributes to the high T_c values, but at the same time it has higher pressure demands. Based on an application perspective, research should focus on how to find superhydrides at moderate pressures. Chen proposed that metal elements with similar atomic radii and electronegativity can form a continuous and homogeneous solid solution, which is beneficial to improving the stability and superconducting properties of the materials.[11] For example, $cP8$-$ScYH_6$ is composed of Sc and Y atoms with similar atomic radii and electronegativity, whose synthesis pathway is via ScH_3 and YH_3. It is dynamically stable at 0.01 GPa with a T_c of about 23 K.[12] While ScH_3 was identified with T_c of about 18.5 K at 131 GPa in experiment[13] and YH_3 was predicted with the maximal T_c of about 40 K at 17.7 GPa.[14] (La, Y)H_6 and (La, Y)H_{10}, with T_c values of 237 K and 253 K, respectively, were synthesized at 170–196 GPa.[15] Notably, according to previous studies, LaH_6 was not thermodynamically stable at high pressures,[16] and YH_{10} was not successfully synthesized at high pressures at least up to 400 GPa.[17]

According to previous studies,[8,9] when the hydrogen content decreases, the stabilizing pressures of the La-H and Y-H phases are reduced considerably, and they can even remain stable at ambient pressure. Meanwhile, the superconducting transition temperature decreases. For example, LaH_2[18] can be stable at ambient pressure but exhibits no superconductivity. In this paper, we select the La–Y–H system with a low hydrogen content and hope these ternary alloy hydrides could perform better superconducting properties under low pressures. We perform structure searches for $LaYH_2$, $LaYH_3$, $LaYH_6$, and $LaYH_8$ in the range of 0–200 GPa and finally find two stable phases for $LaYH_2$ ($C2/m$ and $Pmmn$), and three stable/metastable phases for $LaYH_3$ ($C2/m$, $P2_1/m$ and $R3m$),

[†]Corresponding author. E-mail: chenyangmei@jxust.edu.cn
© 2024 Chinese Physical Society and IOP Publishing Ltd

$LaYH_6$ ($P4_32_12$, $P4/mmm$ and $Cmcm$) and $LaYH_8$ ($P1$, $Imma$ and $P4/mmm$). Finally, the electronic properties and superconductivity of the metallic phase are studied.

2. Computational details

Searches for stable structures of $LaYH_x$ ($x = 2$, 3, 6, 8) with 1–4 formula units in simulation models are performed using the particle swarm optimization methodology as implemented the CALYPSO crystal prediction method.[19,20] The plane-wave basis projector-augmented-wave (PAW) method[21] in the framework of density functional theory (DFT) as implemented in the Vienna *Ab initio* Simulation Package (VASP)[22] is used to perform structural relaxation and electronic property calculations. The Perdew–Burke–Ernzerh (PBE)[23] of the generalized gradient approximation (GGA) is adopted as the exchange–correlation generalized function between the electrons and the $5s^25p^65d^16s^2$ of La, $4s^24p^64d^15s^2$ of Y and $1s^1$ of H are treated as valence electrons for the PAW pseudopotentials. The phonon spectra, electron–phonon coupling parameters and superconducting transition temperatures are calculated using the QUANTUM-ESPRESSO package.[24]

3. Results and discussion

3.1. Phase stability

The pressure dependent formation enthalpies for each structure of $LaYH_x$ ($x = 2$, 3, 6 and 8) are plotted in Fig. 1. The thermodynamic stability is determined by their decompositions with respect to LaH_2,[18] LaH_3,[25] YH_2,[25] YH_3,[16] La,[26] H_2[27] and Y,[28,29] respectively. As shown in Fig. 1, $LaYH_2$ stabilizes in the $C2/m$ phase at 40 GPa and transforms to the $Pmmn$ phase at 67 GPa. For $LaYH_3$, the $C2/m$ phase stabilizes at ambient pressure and transforms to the $P2_1/m$ phase at 12 GPa. As pressure further increases, the $P2_1/m$ phase transforms to the $R3m$ phase at 87 GPa. For $LaYH_6$, the $P4_32_12$ phase stabilizes at ambient pressure and transforms to the $P4/mmm$ phase at 28 GPa, and then to the $Cmcm$ phase at 79 GPa. For $LaYH_8$, the $Imma$ phase stabilizes at 60 GPa and transforms to the $P4/mmm$ phase at 117 GPa. All the stable compounds remain stable up to at least 200 GPa.

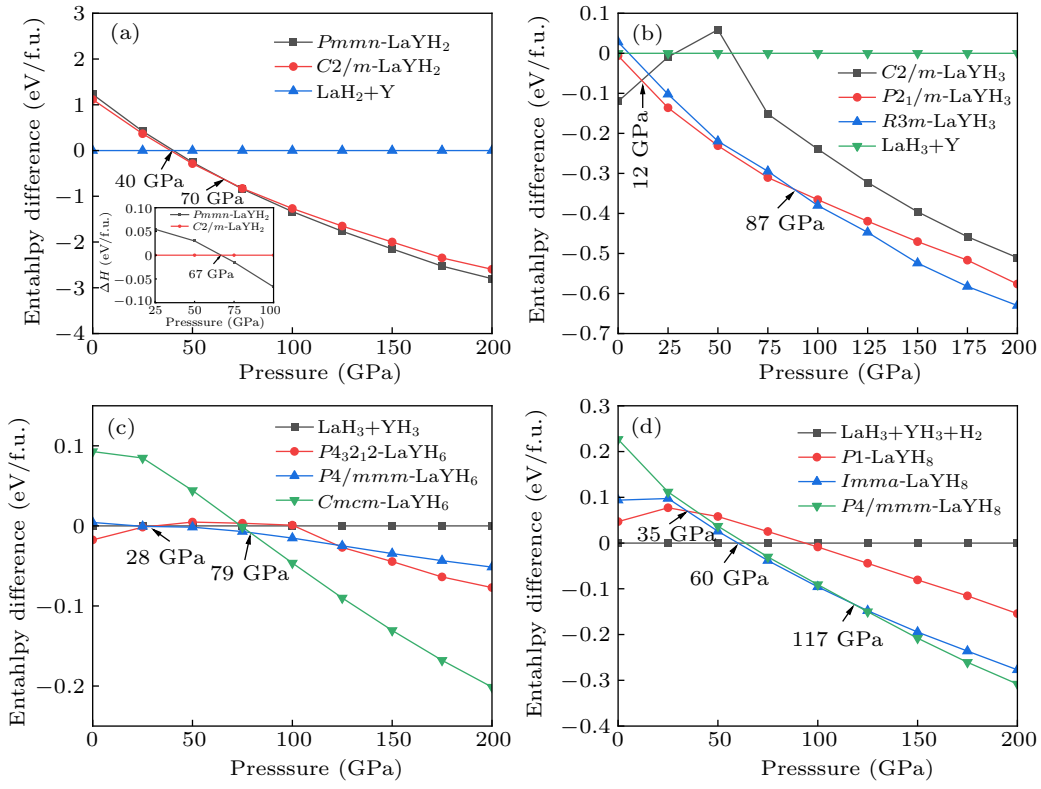


Fig. 1. Pressure dependence of formation enthalpy of (a) $LaYH_2$, (b) $LaYH_3$, (c) $LaYH_6$ and (d) $LaYH_8$. The inset of (a) shows the pressure dependent formation enthalpy for $C2/m$-$LaYH_2$ and $Pmmn$-$LaYH_2$ under 25–100 GPa.

In addition, we have calculated the phonon dispersion curves of each phase of $LaYH_2$, $LaYH_3$, $LaYH_6$ and $LaYH_8$ to determine their dynamical stability. As shown in Fig. 2, there are no imaginary frequencies in the phonon dispersion curves of all the structures at certain pressures, indicating that they are dynamically stable. Notably, the $C2/m$-$LaYH_2$ and $P1$-$LaYH_8$ which have positive formation enthalpies (thermodynamically unstable) at ambient pressure are dynamically stable, which means that they are possible to keep metastable at ambient pressure.

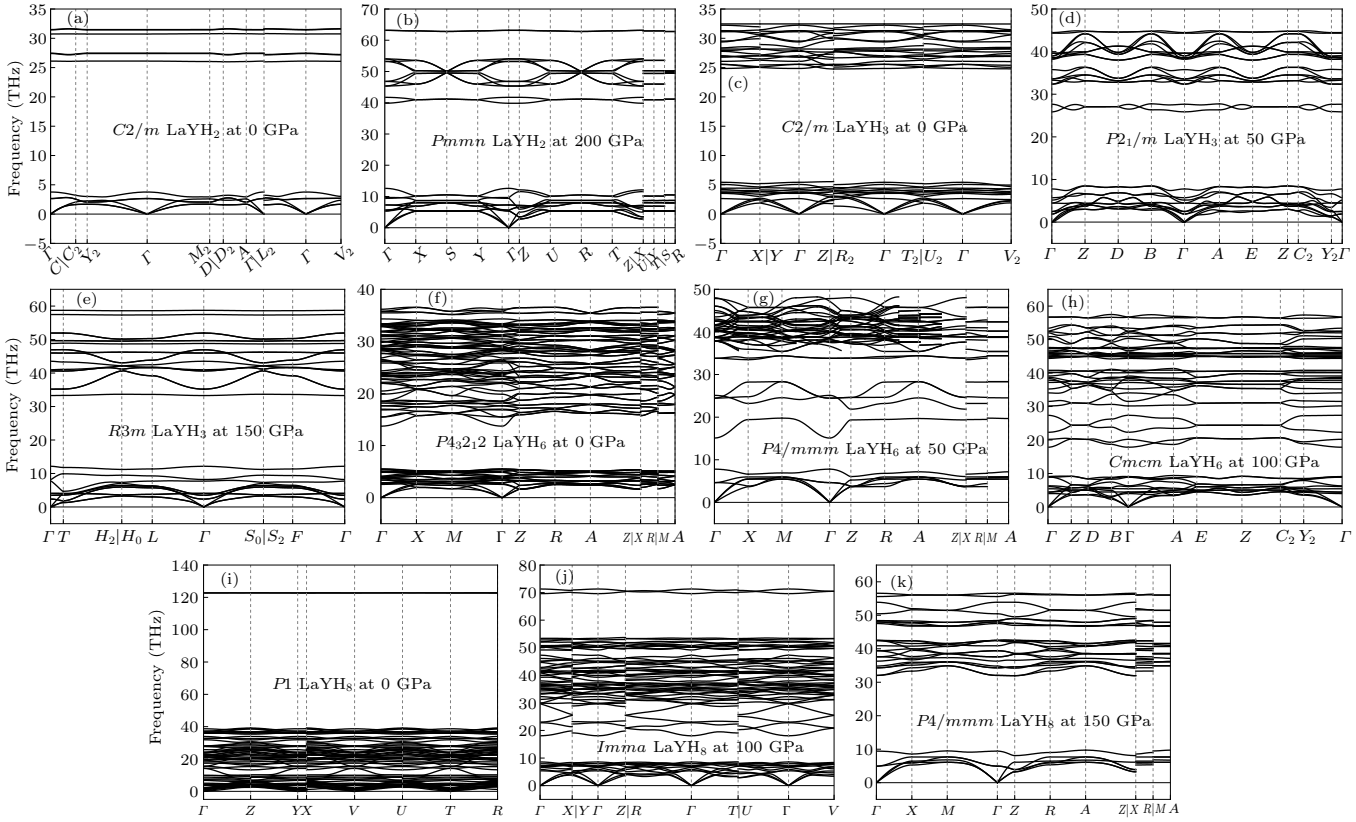


Fig. 2. Phonon dispersion curves of different phases at certain pressures.

3.2. Crystal structure and chemical bonding

The crystal structures for each phase of $LaYH_2$, $LaYH_3$, $LaYH_6$ and $LaYH_8$ are shown in Fig. 3. For $LaYH_2$, the $C2/m$ phase has a monoclinic symmetry in which the Y atom is surrounded by six H atoms, forming a YH_6 unit. YH_6 unit extends in a direction perpendicular to the c-axis, and La atoms connect the different layers of YH_6. The $Pmmn$ phase has an orthorhombic symmetry in which each La atom is attached to one H atom and each Y atom is connected to four H atoms, forming YH_4 units. The shortest H–H distances are 2.58 Å at ambient pressure and 1.63 Å at 200 GPa in $C2/m$- and $Pmmn$-$LaYH_2$, which are much longer than the H–H bond length in the H_2 molecule.[27] In the $C2/m$ phase of $LaYH_3$, each La and Y atom is surrounded by six H atoms, forming LaH_6 and YH_6 units, which distribute in a stacking pattern along the direction perpendicular to the (001) crystal plane. In the $P2_1/m$ phase with monoclinic symmetry, each La and Y atom forms LaH_5 and YH_5 units with five H atoms. In the $R3m$ phase with tripartite symmetry, each La atom forms LaH_4 unit with four H atoms, and the Y atoms form YH_6 and YH_3 units with six and three H atoms, respectively. The shortest H–H distances for $C2/m$, $P2_1/m$, and $R3m$ phases are 2.42 Å at ambient pressure, 2.11 Å at 50 GPa, and 1.57 Å at 150 GPa, respectively.

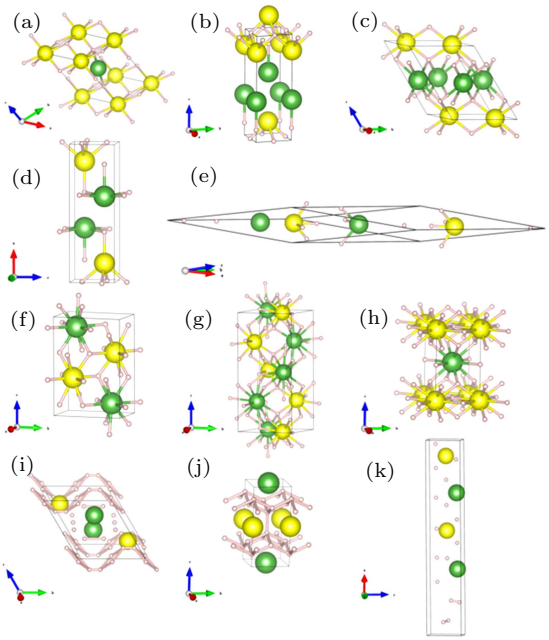


Fig. 3. The predicted crystal structures of ternary hydrides under pressure: (a) $C2/m$-$LaYH_2$ at 0 GPa, (b) $Pmmn$-$LaYH_2$ at 200 GPa, (c) $C2/m$-$LaYH_3$ at 0 GPa, (d) $P2_1/m$-$LaYH_3$ at 150 GPa, (e) $R3m$-$LaYH_3$ at 50 GPa, (f) $Cmcm$-$LaYH_6$ at 0 GPa, (g) $P4_32_12$-$LaYH_6$ at 50 GPa, (h) $P4/mmm$-$LaYH_6$ at 100 GPa, (i) $Imma$-$LaYH_8$ at 100 GPa, (j) $P4/mmm$-$LaYH_8$ at 200 GPa, and (k) $P1$-$LaYH_8$ at 0 GPa. Green, yellow and pink balls represent La, Y and H atoms, respectively.

For $LaYH_6$, the $P4_32_12$ phase has a tetragonal symmetry in which La and Y atoms are surrounded by 11 and 10 H atoms, respectively, forming LaH_{11} and YH_{10} units. These units are connected by a shared H atom. The $P4/mmm$ phase is a body-centered tetragonal structure. La and Y atoms are surrounded by 12 H atoms to form YH_{12} and LaH_{12} units, which are stacked along the c-axis. The $Cmcm$ phase has an orthorhombic symmetry in which La and Y atoms are sur-

rounded by 10 H atoms to form YH_{10} and LaH_{10} units. The shortest H–H distances for the $P4_32_12$, $P4/mmm$, and *Cmcm* phases are 2.20 Å at ambient pressure, 2.03 Å at 50 GPa, and 1.62 Å at 100 GPa, respectively. For $LaYH_8$, the shortest H–H distances are 0.78 Å in the $P1$ phase at ambient pressure, and 0.89 Å in the *Imma* phase at 100 GPa, and 1.45 Å in the $P4/mmm$ phase at 200 GPa, respectively. The above results indicate that as the hydrogen content increases in the La–Y–H system, the shortest H–H distances decrease and the covalent H–H interactions form.

The electron localization functions (ELFs) for each structure of $LaYH_2$, $LaYH_3$, $LaYH_6$, and $LaYH_8$ are shown in Fig. 4. The calculated ELF values between the H atoms are less than 0.5 in all structures of $LaYH_2$, $LaYH_3$ and $LaYH_6$, revealing no covalent interactions between the H atoms. For $LaYH_8$, there is strong electronic localization with ELF values close to 1 between some of the hydrogen atoms in the $P1$ and *Imma* phases. The $P4/mmm$ phase contains weakly covalent hydrogen atoms (ELF value of approximately 0.6) and isolated hydrogen ions. Bader charge analyses[30] show that there is a large amount of charge transfer from La and Y atoms to H atoms.

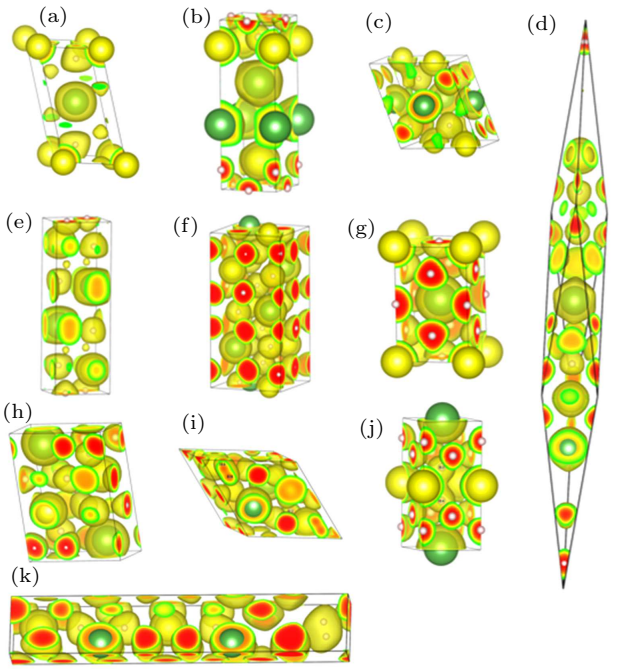


Fig. 4. The electronic localization function of (a) $C2/m$-$LaYH_2$ at 0 GPa, (b) $Pmmn$-$LaYH_2$ at 200 GPa, (c) $C2/m$-$LaYH_3$ at 0 GPa, (d) $P2_1/m$-$LaYH_3$ at 150 GPa, (e) $R3m$-$LaYH_3$ at 50 GPa, (f) $Cmcm$-$LaYH_6$ at 0 GPa, (g) $P4_32_12$-$LaYH_6$ at 50 GPa, (h) $P4/mmm$-$LaYH_6$ at 100 GPa, (i) *Imma*-$LaYH_8$ at 100 GPa, (j) $P4/mmm$-$LaYH_8$ at 200 GPa, and (k) $P1$-$LaYH_8$ at 0 GPa.

3.3. Electronic properties

To analyze the electronic properties, the electronic band structure and density of states (DOS) are calculated. As displayed in Fig. 5, all of the stable phases of $LaYH_2$ and $LaYH_3$ have bands crossing the Fermi level, indicating that these phases are metallic. The states at the Fermi level of each phase are dominated by the metal atoms La and Y, and the contribution from H atoms is negligible. This situation resembles LaH_2 and YH_2.[31] This violates one of the essential criteria in searching of high-T_c superconducting hydride: a large value of H-derived DOS at the Fermi level,[32] which is always associated with a strong electron–phonon interaction. Therefore, it is unfavorable for the superconductivity of $LaYH_2$ and $LaYH_3$. The same situation also occurs in La_2N_2H,[33] where the electronic density of states at the Fermi level is dominated by La and N, exhibiting metallicity but with T_c values less than 1 K.

For $LaYH_6$, the $P4_32_12$ phase is a semiconductor with a direct band gap of 1.49 eV at 0 GPa. The *Cmcm* and $P4/mmm$ phases are both weakly metallic with small DOS values at the Fermi level at 50 GPa and 100 GPa, respectively. For $LaYH_8$, the $P1$ phase (metastable) is also a semiconductor with a direct band gap of 0.91 eV at 0 GPa. The *Imma* and $P4/mmm$ phases are metallic at 100 GPa and 150 GPa, respectively. In contrast to the other phases in the La–Y–H system, $P4/mmm$-$LaYH_8$ has a relatively large value of H-derived DOS at the Fermi level, suggesting that it may be a potential superconductor.

3.4. Superconductivity

Considering the metallic nature of $LaYH_2$, $LaYH_3$ and $LaYH_8$, we further calculate their electron–phonon coupling parameters to estimate the superconducting temperature T_c by using the Allen–Dynes modified McMillan equation.[34] The electron–phonon coupling constant λ and the logarithmic average frequency ω_{log} are two important parameters that determine the T_c value. As shown in Table 1, both $LaYH_2$ and $LaYH_3$ have weak electron–phonon coupling and low values of ω_{log}, which therefore lead to low superconducting transition temperatures. The T_c values of $C2/m$-$LaYH_2$ and $C2/m$-$LaYH_3$ at ambient pressure are less than 1 K. And the $Pmmn$-$LaYH_2$, $R3m$-$LaYH_3$ and $P2_1/m$-$LaYH_3$ have T_c values of 1.57 K, 3.64 K and 5.22 K at 100 GPa, 150 GPa, and 50 GPa, respectively. For $LaYH_8$, the values of λ and ω_{log} of the $P4/mmm$ phase are significantly elevated, resulting in a T_c value of 55.51 K at 50 GPa. To further analyze the superconducting mechanism of $P4/mmm$-$LaYH_8$, we plot the frequency dependence of λ and the Eliashberg spectral functions $\alpha^2F(\omega)$ corresponding to the projected phonon density of states in Fig. 6. It is shown that the vibration of H atoms which occupy the high-frequency region above 15 THz contribute mainly (80% at 50 GPa and 73% at 200 GPa) to the total electron–phonon coupling.

Table 1. The calculated electron–phonon coupling parameters λ, the logarithmic average frequency ω_{log}, and superconducting critical temperatures T_c (K) ($u^* = 0.13$) for different phases at different pressures.

Compound	Pressure (GPa)	λ	ω_{log}	T_c (K)
$C2/m$-$LaYH_2$	0	0.43	140	0.47
$Pmmn$-$LaYH_2$	100	0.46	313	1.57
$C2/m$-$LaYH_3$	0	0.26	219	0
$P2_1/m$-$LaYH_3$	50	0.68	206	5.22
$R3m$-$LaYH_3$	150	0.54	324	3.64
	50	1.02	895	55.51
$P4/mmm$-$LaYH_8$	150	0.83	1128	46.96
	200	0.71	1217	34.67

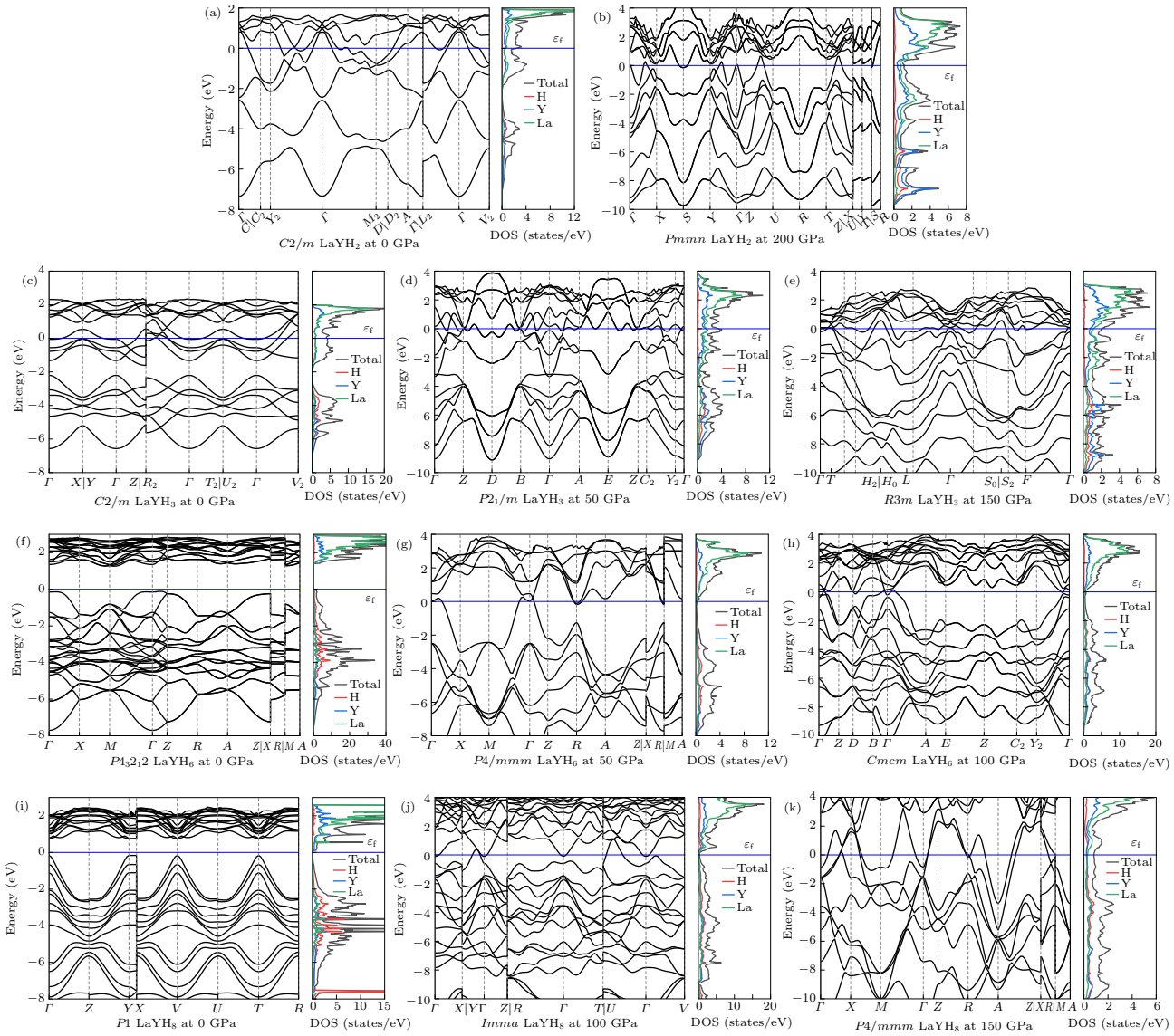


Fig. 5. Electronic band structures and local density of states, the horizontal line indicates the Fermi levels.

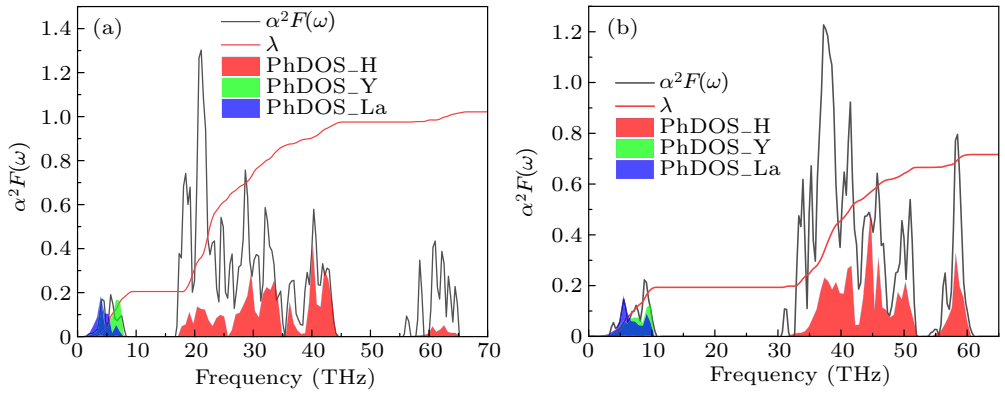


Fig. 6. The Eliashberg spectral functions $\alpha^2F(\omega)$, the projected phonon density of states (PHDOS), and the electron–phonon coupling parameter λ of $P4/mmm$-LaYH$_8$ at (a) 50 GPa and (b) 200 GPa.

4. Conclusion

In summary, we perform a theoretical study on the structure, stability, electronic and superconducting properties of LaYH$_2$, LaYH$_3$, LaYH$_6$, and LaYH$_8$ at pressures of 0–200 GPa. Two stable phases for LaYH$_2$ ($C2/m$ and $Pmmn$) and three stable phases for LaYH$_3$ ($C2/m$, $P2_1/m$ and $R3m$), LaYH$_6$ ($P4_32_12$, $P4/mmm$ and $Cmcm$) and LaYH$_8$ ($P1$, $Imma$ and $P4/mmm$) have been predicted. Remarkably, LaYH$_x$ ($x = 2, 3, 6, 8$) can be stable (or metastable) at ambient pressure. The calculated band structures indicate that all phases

of $LaYH_2$ and $LaYH_3$ predicted here are metallic. In these phases, H exists as ionic H without covalent interactions. The electronic density of states at the Fermi level is dominated by La and Y instead of H, which results in weak electron–phonon coupling interactions and low superconducting temperatures. $LaYH_6$ is a semiconductor at ambient pressure and exhibits poor metallic nature under high pressures. $LaYH_8$ is the only compound which has substantial electron–phonon coupling interactions. The calculated T_c value of $P4/mmm$-$LaYH_8$ is 55.51 K at 50 GPa.

Acknowledgements

Project supported by the National Natural Science Foundation of China (Grant Nos. 12364003, 11804131, 11704163, 12375014, and 11875149) and the Natural Science Foundation of Jiangxi Province of China (Grant Nos. 20232BAB211022 and 20181BAB211007).

References

[1] Bardeen J, Cooper L N and Schrieffer J R 1957 *Phys. Rev.* **108** 1175
[2] McMahon J M and Ceperley D M 2011 *Phys. Rev. Lett.* **106** 165302
[3] Ashcroft N W 2004 *Phys. Rev. Lett.* **92** 187002
[4] Duan D, Liu Y, Tian F, Li D, Huang X, Zhao Z, Yu H, Liu B, Tian W and Cui T 2014 *Sci. Rep.* **4** 6968
[5] Drozdov A P, Eremets M I, Troyan I A, Ksenofontov V and Shylin S I 2015 *Nature* **525** 73
[6] Li B, Yang Y, Fan Y, Zhu C, Liu S and Shi Z 2023 *Chin. Phys. Lett.* **40** 097402
[7] Flores-Livas J A, Boeri L, Sanna A, Profeta G, Arita R and Eremets M 2020 *Phys. Rep.* **856** 1
[8] Wang H, Tse J S, Tanaka K, Iitaka T and Ma Y 2012 *Proc. Nat. Acad. Sci. USA* **109** 6463
[9] Drozdov A P, Kong P P, Minkov V S, Besedin S P, Kuzovnikov M A, Mozaffari S, Balicas L, Balakirev F F, Graf D E, Prakapenka V B, Greenberg E, Knyazev D A, Tkacz M and Eremets M I 2019 *Nature* **569** 528
[10] Troyan I A, Semenok D V, Kvashnin A G, Sadakov A V, Sobolevskiy O A, Pudalov V M, Ivanova A G, Prakapenka V B, Greenberg E, Gavriliuk A G, Lyubutin I S, Struzhkin V V, Bergara A, Errea I, Bianco R, Calandra M, Mauri F, Monacelli L, Akashi R and Oganov A R 2021 *Adv. Mater.* **33** 2006832
[11] Chen W, Huang X, Semenok D V and Cui T 2023 *Nat. Commun.* **14** 2660
[12] Wei Y K, Jia L Q, Fang Y Y, Wang L J, Qian Z X, Yuan J N, Selvaraj G, Ji G F and Wei D Q 2021 *Int. J. Quantum Chem.* **121** e26459
[13] Shao M, Chen S, Chen W, Zhang K, Huang X and Cui T 2021 *Inorg. Chem.* **60** 15330
[14] Li Y, Hao J, Liu H, Tse J S, Wang Y and Ma Y 2015 *Sci. Rep.* **5** 9948
[15] Semenok D V, Troyan I A, Ivanova A G, Kvashnin A G, Kruglov I A, Hanfland M, Sadakov A V, Sobolevskiy O A, Pervakov K S, Lyubutin I S, Glazyrin K V, Giordano N, Karimov D N, Vasiliev A L, Akashi R, Pudalov V M and Oganov A R 2021 *Mat. Today* **48** 18
[16] Peng F, Sun Y, Pickard C J, Needs R J, Wu Q and Ma Y 2017 *Phys. Rev. Lett.* **119** 107001
[17] Kong P, Minkov V S, Kuzovnikov M A, Drozdov A P, Besedin S P, Mozaffari S, Balicas L, Balakirev F F, Prakapenka V B, Chariton S, Knyazev D A, Greenberg E and Eremets M I 2021 *Nat. Commun.* **12** 5075
[18] He D C, Shao H X and Wei Y K 2015 *Can. J. Phys.* **93** 1630
[19] Wang Y, Lv J, Zhu L and Ma Y J P R B 2010 *Phys. Rev. B* **82** 094116
[20] Wang Y, Lv J, Zhu L and Ma Y 2012 *Comput. Phys. Commun.* **183** 2063
[21] Blöchl P E 1994 *Phys. Rev. B* **50** 17953
[22] Kresse G and Furthmüller J 1996 *Phys. Rev. B* **54** 11169
[23] Perdew J P, Burke K and Ernzerhof M J 1996 *Phys. Rev. Lett.* **77** 3865
[24] Giannozzi P, Baroni S, Bonini N, Calandra M, Car R, Cavazzoni C, Ceresoli D, Chiarotti G L, Cococcioni M, Dabo I, Dal Corso A, de Gironcoli S, Fabris S, Fratesi G, Gebauer R, Gerstmann U, Gougoussis C, Kokalj A, Lazzeri M, Martin-Samos L, Marzari N, Mauri F, Mazzarello R, Paolini S, Pasquarello A, Paulatto L, Sbraccia C, Scandolo S, Sclauzero G, Seitsonen A P, Smogunov A, Umari P and Wentzcovitch R M 2009 *J. Phys.: Condens. Matter* **21** 395502
[25] Liu H, Naumov I I, Hoffmann R, Ashcroft N W and Hemley R J 2017 *Proc. Natl. Acad. Sci. USA* **114** 6990
[26] Spedding F H, Daane A and Herrmann K J 1956 *Acta Crystal.* **9** 559
[27] Pickard C J and Needs R J 2007 *J. New Phys.* **3** 473
[28] Chen Y, Hu Q M and Yang R 2011 *Phys. Rev. B* **84** 132101
[29] Chen Y, Hu Q M and Yang R 2012 *Phys. Rev. Lett.* **109** 157004
[30] Bader R F 1990 *Atoms in molecules*, Wiley Online Library
[31] Yang J W, Gao T and Guo L Y 2013 *Physica B* **429** 119
[32] Lv J, Sun Y, Liu H and Ma Y 2020 *Matter Radiat. Extrem.* **5** 068101
[33] Di Cataldo S, von der Linden W and Boeri L 2022 *npj Comput. Mater.* **8** 2
[34] Allen P B and Dynes R C 1975 *Phys. Rev. B* **12** 905